Molecular Microbiology (2014) 92(1), 47–60 ■
doi:10.1111/mmi.12536
First published online 6 March 2014

OmpA and OmpC are critical host factors for bacteriophage Sf6 entry in *Shigella*

Kristin N. Parent,[1,2*] Marcella L. Erb,[3] Giovanni Cardone,[2] Katrina Nguyen,[3] Eddie B. Gilcrease,[4] Natalia B. Porcek,[1,5] Joe Pogliano,[3] Timothy S. Baker[2,3] and Sherwood R. Casjens[4]

Departments of [1]Biochemistry and Molecular Biology and [5]Microbiology and Molecular Genetics, Michigan State University, East Lansing, MI 48824, USA.
[2]Department of Chemistry & Biochemistry and [3]Division of Biological Sciences, University of California, San Diego, La Jolla, CA 92093, USA.
[4]Division of Microbiology and Immunology, Department of Pathology, University of Utah School of Medicine, Salt Lake City, UT 84112, USA.

Summary

Despite being essential for successful infection, the molecular cues involved in host recognition and genome transfer of viruses are not completely understood. Bacterial outer membrane proteins A and C co-purify in lipid vesicles with bacteriophage Sf6, implicating both outer membrane proteins as potential host receptors. We determined that outer membrane proteins A and C mediate Sf6 infection by dramatically increasing its rate and efficiency. We performed a combination of *in vivo* studies with three *omp* null mutants of *Shigella flexneri*, including classic phage plaque assays and time-lapse fluorescence microscopy to monitor genome ejection at the single virion level. Cryo-electron tomography of phage 'infecting' outer membrane vesicles shows the tail needle contacting and indenting the outer membrane. Lastly, *in vitro* ejection studies reveal that lipopolysaccharide and outer membrane proteins are both required for Sf6 genome release. We conclude that Sf6 phage entry utilizes either outer membrane proteins A or C, with outer membrane protein A being the preferred receptor.

Accepted 30 January, 2014. *For correspondence. E-mail kparent@msu.edu; Tel. (+1) 517 432 8434; Fax (+1) 517 353 9334.

Introduction

Non-enveloped viruses include the vast majority of bacteriophages and many human pathogens. Despite their widespread occurrence and medical relevance, the molecular mechanisms that govern their genome delivery are not completely understood. Productive infection requires precise docking to a designated location on the cell surface to enable delivery of the viral genome through several steps that may include: initial specific recognition of the cell surface through interaction with a 'primary' host receptor, 'triggering' the process of nucleic acid release from the virion (e.g. by receptor recognition), followed by co-ordinated conformational changes in viral proteins, and ultimately genome transfer into the target cell. Such transfer is a universal phenomenon among viruses and must be highly regulated since evolutionary pressures demand that errors leading to premature or inappropriate release be avoided. Although the genomes of viruses must breach or transit through a wide variety of obstacles such as bacterial cell walls, some common strategies and mechanisms are utilized (Poranen *et al.*, 2002). Receptor-binding proteins in viruses are needed to attach to the outside of the host cell, and these can have conserved structures. For example, cell receptor-binding proteins of PRD-1 (infects a range of Gram-negative bacteria such as *Pseudomonas aeruginosa*, *Escherichia coli*, *Vibrio cholera*, and *Salmonella typhimurium*) and adenoviruses (infects humans) share a common polypeptide fold (Bamford *et al.*, 2005). Another common theme is that ion-permeable pores facilitate genome translocation as occurs in diverse viral systems such as tailed bacteriophage and poliovirus (Poranen *et al.*, 2002).

Bacteriophage Sf6 is a short-tailed dsDNA virus (family *Podoviridae*) that infects *Shigella flexneri*, a causative agent of bacillary dysentery. *Shigella*, the third most prevalent bacterial food-borne pathogen (Warren *et al.*, 2006), is responsible for over 165 million human cases of dysentery worldwide each year (Kotloff *et al.*, 1999). Although most *Shigella* infections are reported in underdeveloped countries, the disease has become more widespread in recent years (Feil, 2012; Holt *et al.*, 2012). Interactions between phage Sf6 and its host can result in altered host pathogenicity by changing its surface characteristics, such as via an acetylase that affects the O-antigen polysaccharide of

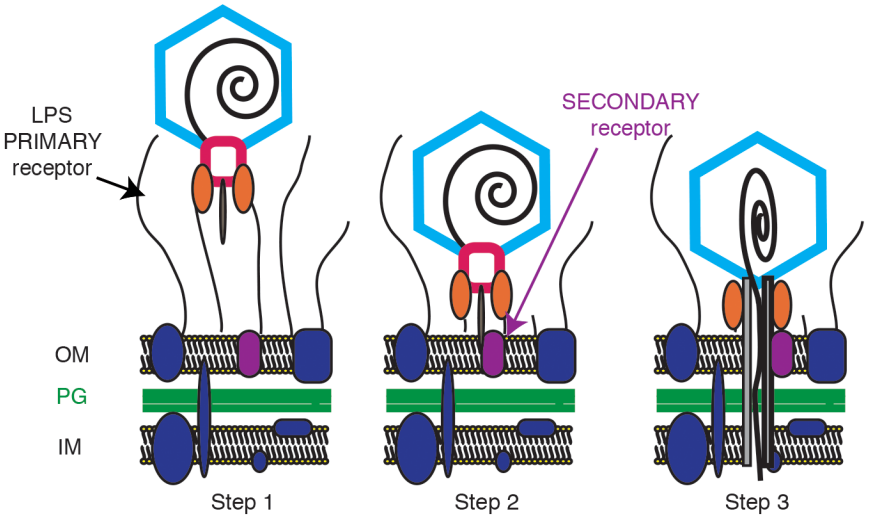

Fig. 1. Schematic diagram of steps in dsDNA genome ejection for members of the family *Podoviridae*. Step 1: A virion binds to its cell surface primary receptor. In the P22-like phages, the phage tailspike proteins (orange ovals) bind the lipopolysaccharide (LPS) through the O-antigen. Step 2: Tailspike proteins hydrolyse the LPS and the virion moves closer to the cell surface where it can now bind a putative secondary receptor. Step 3: dsDNA likely enters the cell through a channel formed by phage 'ejection' proteins (P22 releases three proteins, gp7, gp16, and gp20 during DNA release). OM, outer membrane; PG, peptidoglycan; IM, inner membrane. This schematic was modified from Casjens and Molineux (2012).

lipopolysaccharide (LPS) (Clark *et al*., 1991; Verma *et al*., 1991). Therefore, a more detailed understanding of host recognition and infection mechanisms is needed (Allison and Verma, 2000; Banks *et al*., 2002; Broadbent *et al*., 2010). In many tailed phages, short, thick fibres ('tailspike proteins') are responsible for initial interaction with LPS (the 'primary' receptor) and mediate reversible cell binding (Fig. 1, step 1). Sf6 is a member of the P22-like group of tailed phages, which includes over 150 phages and prophages that have similar sets of virion assembly genes (Casjens and Thuman-Commike, 2011), and tailspikes of this phage group bind to and cleave the surface O-antigen of their host LPS. Atomic-resolution structures are available for P22 and Sf6 tailspike proteins (Steinbacher *et al*., 1997; Muller *et al*., 2008), and these are strikingly similar despite having no recognizable similarity in amino acid sequence (Baxa *et al*., 1996; Chua *et al*., 1999). Purified LPS of *Salmonella enterica* serovar Typhimurium is sufficient to cause a slow release of the P22 genome *in vitro* (Andres *et al*., 2010), but it is unclear if LPS alone is sufficient to induce rapid and accurate genome release *in vivo*. Secondary receptors (i.e. those that often mediate irreversible cell binding) are necessary for infection by a number of other phages and the presence of secondary receptors in *Podoviridae*, including N4, has been reported (Kiino *et al*., 1993; McPartland and Rothman-Denes, 2009).

Many diverse Gram-negative bacteria, including *Shigella*, secrete outer membrane vesicles (OMVs) (Berlanda Scorza *et al*., 2012), and OMV production can increase in response to attack by lytic phages (Kulp and Kuehn, 2010). Previously, host-derived outer membrane proteins (Omps) A and C were reported to co-purify with Sf6, even after CsCl purification, through OMVs attached to the Sf6 tail machinery (Zhao *et al*., 2011; Parent *et al*., 2012). The tight association of Sf6 with OMVs indicates that Sf6 and P22 may differ in their binding to hosts since OMVs do not co-purify with P22. In the present study we investigated the roles of *S. flexneri* OmpA and OmpC during Sf6 infection, and demonstrate that both Omps act as secondary receptors and increase Sf6 genome ejection efficiency. Our results suggest that host recognition and genome transfer follow diverse pathways even within rather closely related phages.

Results

Sf6 plating efficiency is reduced in the absence of host OmpA and OmpC

Three null mutants of *S. flexneri* were created to investigate the role of Omps A and C during the initial stages of Sf6 infection. Two of the mutants contain single gene knockouts (*ompA*$^-$ and *ompC*$^-$) as described previously (Parent *et al*., 2012), and the third strain lacks both genes (*ompA*$^-$*C*$^-$, constructed as described in *Supporting information*). We compared Sf6 growth on and infection of wild-type (WT) *Shigella* with these three null mutants to explore how OmpA and OmpC affect phage growth. For all experiments described herein, the Sf6 phage carried a

clear mutation that blocks lysogen formation (Casjens *et al*., 2004). Sf6 plaque morphology differed between the WT and each of the three *omp* knockout strains (Supplementary Materials, Fig. S1A). The efficiency of Sf6 plating was determined on the *omp* defective hosts relative to the WT host at a range of temperatures between 20°C and 42°C. Sf6 plating efficiency was essentially the same on WT and the *ompA*$^-$ and *ompC*$^-$ single knockout hosts. However, at all temperatures it was ~10-fold or more lower when Sf6 was plated on the *ompA*$^-$*C*$^-$ strain (Fig. S1B).

Sf6 kills WT S. flexneri *cells more efficiently than cells lacking OmpA and OmpC*

A decrease in plating efficiency (Fig. S1B) on the double *S. flexneri ompA*$^-$*C*$^-$ null strain could result from one of two possibilities. Either the phage is unable to recognize and infect the mutant cells, or infection occurs but no progeny are produced [as was suggested by work that proposed OmpA and OmpC are incorporated into virions as a means of stabilization (Zhao *et al*., 2011)]. To determine which of these possibilities accounts for the observed decrease, we performed a cell survival assay. In this experiment, mid-logarithmically growing cells at 2×10^8 cells ml^{-1} were incubated at increasing multiplicity of infection (moi, the number of phage added per cell) of Sf6 at 30°C. Resulting colonies were counted and relative survival values were calculated as the number of colony-forming units (cfu) at each moi divided by the number of cfu present prior to infection (Fig. S2). The colonies represent cells that have not been infected, since infected *Shigella* cells do not survive Sf6 clear mutant infection. For the WT strain, an moi of two was sufficient to reduce the *Shigella* population by more than half, and the relative survival decreased as the moi of Sf6 increased. These results are consistent with similar experiments performed using *Salmonella enterica* serovar Typhimurium infected by phage P22 (Gordon, 1993). The *ompC*$^-$ host demonstrated a very slight change in cell survival compared to WT, whereas the *ompA*$^-$ host showed a larger, and statistically significant increase. The *ompA*$^-$*C*$^-$ host had the highest level of survival at all moi and required four to five times more phage to achieve the same killing as in the WT host.

Sf6 infection is slower in S. flexneri *that lack both OmpA and OmpC*

Single step growth curve experiments obtain information about the rates of phage absorption to the host as well as the rates and amounts ('burst size') of phage produced per cell. Sf6 phage were added to mid-logarithmically growing cells at an moi that ensured > 95% of the cells were infected in each experiment. The phage/cell ratio at each time point was calculated by dividing the number of viable phage (an aliquot of the infected culture was titred post chloroform-induced lysis and immediate dilution) by the number of cells present in the initial culture. For WT *Shigella*, the observed plaque-forming units (pfu) per cell decreases rapidly as the phage attach to the host cells, inject their genomes, and enter the eclipse phase. The pfu per cell subsequently increases as progeny phage are produced, until reaching steady-state at approximately 60 min post-infection. The growth curve kinetics and burst size for Sf6 in WT *Shigella* are similar to those reported for P22 in *Salmonella* (Botstein *et al*., 1973; Aramli and Teschke, 1999). Compared to the curves obtained for WT *S. flexneri*, Sf6 growth curves were altered for all three *omp* null mutant strains highlighting the relative changes in DNA delivery when Omps are absent. The rate of infection decreased slightly on *ompC*$^-$, whereas infection dropped by an order of magnitude on *ompA*$^-$ (Fig. 2A). For *ompA*$^-$*C*$^-$, infection was significantly slower and was several orders of magnitude lower (Fig. 2A). Nevertheless, the relative rates of progeny phage formation and relative burst sizes were similar in all strains, indicating that Omps A and C affected the initial infection step but did not alter phage production once the cells were infected. In addition, we repeated the experiment above with the exception of not artificially rupturing the cells via chloroform to determine the minimum time to lysis as well as the average rise time for each strain. Minimum time to lysis from onset of Sf6 addition at 30°C occurs as follows: WT = 63 min; *ompA*$^-$ = 76 min; *ompC*$^-$ = 65 min; *ompA*$^-$*C*$^-$ = 78 min (data are averaged from three experiments and the error was ± 3 min). The average rise time once lysis had initiated was similar for all strains (~ 45 min).

Initial rates of Sf6 reversible adsorption to WT and *omp* null *Shigella* were monitored by adding phage to cells, taking aliquots at various times, spinning out the cells and attached phage, and titring the supernatant. This experiment allowed us to determine the number of unadsorbed phage as a function of time, and thus calculate the rate of Sf6 adsorption to LPS under a variety of conditions. Representative data are shown for Sf6 adsorbing to WT *Shigella* (Fig. 2B). For each strain, adsorption rates were calculated from 8 to 11 different concentrations of cells and were plotted as a function of cell concentration for each strain (Fig. 2C). There are no substantial differences between the strains, indicating that initial, reversible interaction with LPS is not varied as a result of the *omp* deletions. Therefore, the relative differences that we observed in the eclipse phase in our single step growth curves (Fig. 2A) is independent of LPS adsorption rate, and is most likely owing to a slower irreversible adsorption step from the lack of Omps A and C.

Why is the eclipse phase slightly altered in *ompC*$^-$ and *ompA*$^-$ and dramatically altered on the *ompA*$^-$*C*$^-$ host? Removal of OmpA and OmpC may have a pleiotropic or negative effect on cells, and slower eclipse phases could

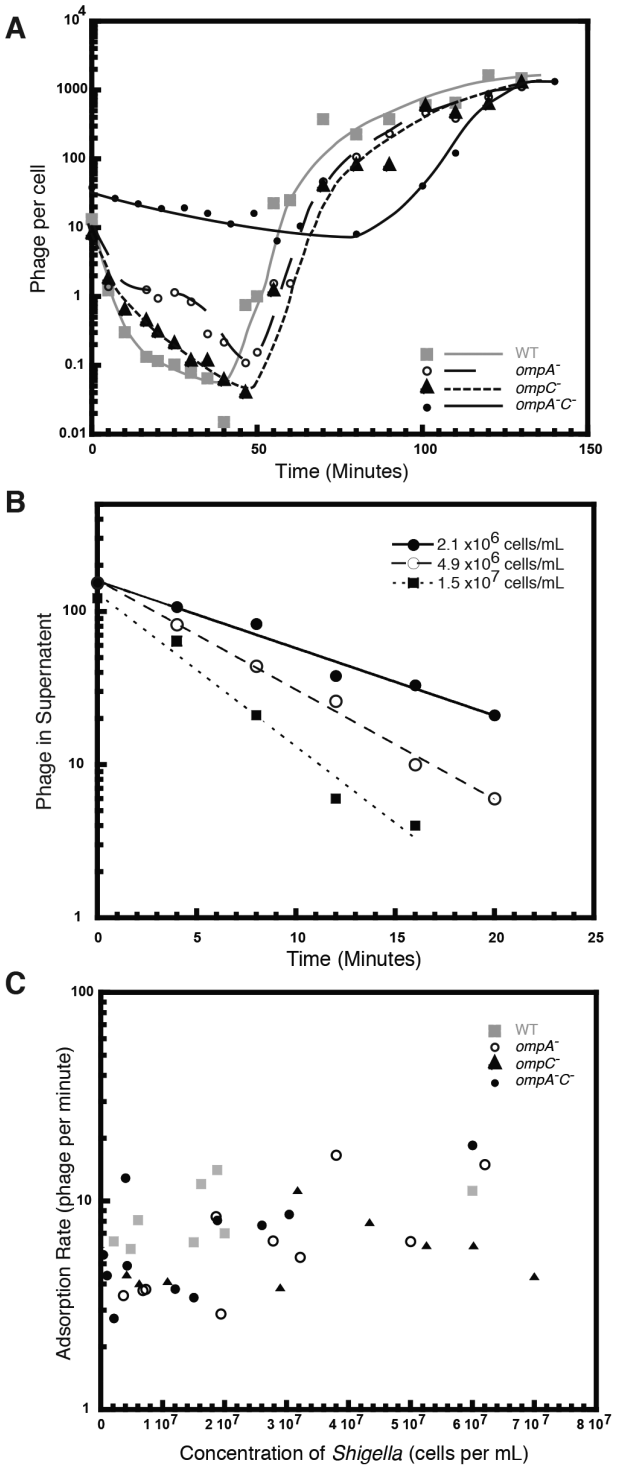

Fig. 2. Sf6 infection is slowest in *ompA*$^{-}$*C*$^{-}$ *Shigella*.
A. Exponentially growing *Shigella* were infected with Sf6 phage and at the designated times after infection, aliquots of each reaction were treated with chloroform and plated at 30°C on WT *Shigella*. The number of phage per cell was calculated as the titre of phage at each time point divided by the total number of cells in the reaction. Each growth curve was repeated in triplicate, and representative plots are shown.
B. Representative plots of reversible Sf6 adsorption rates to WT cells.
C. Reversible adsorption rates of Sf6 to WT and the three omp null *Shigella* hosts are plotted as a function of cell concentration and do not differ significantly between WT and the *omp* null hosts.

be unrelated to secondary receptor binding, but instead influenced by the overall health of the *omp* mutant strains. For example, if the *omp* deletions alter production of the primary receptor (O-antigen portion of LPS), the phage would also show changes in adsorption (Gemski *et al*., 1975). To test this possibility, we performed LPS extractions of each *S. flexneri* strain and found no discernable differences in the amount of LPS present or in O-antigen length as measured by silver staining tris-tricine gels displaying the isolated LPS (data not shown). This result is consistent with a previous LPS analysis of *S. flexneri* strain HND92, which carries a different *ompA* deletion mutant (Ambrosi *et al*., 2012). Therefore, phage likely bind the LPS of the *omp* null cells in a normal manner (Fig. 1, step 1). A second possibility is that *omp* deletion may affect outer membrane integrity. We tested growth of all four strains on MacConkey agar, a bile-salt-rich media that selects for Gram-negative bacteria with an intact outer membrane (MacConkey, 1905). All four strains grew on MacConkey plates (data not shown) indicating that the outer membranes were intact.

Time-lapse fluorescence microscopy shows that Sf6 infection is slower in omp *null mutants*

We used time-lapse fluorescence microscopy to monitor phage Sf6 infection of *Shigella* and visualize real-time genome translocation at the single virion level at 20°C (Fig. 3). Sf6 virions were stained with Sytox green since it penetrates capsids but not live cells (Langsrud and Sundheim, 1996; Roth *et al*., 1997). Images were recorded every 3 min after initiation of infection (see *Experimental procedures*). Phage particles attached to cells appeared as bright green foci immediately adjacent to the cells (Fig. 3A). Transfer of phage DNA into the host cell was observed directly as a decrease in fluorescence of the phage particle and the simultaneous emergence of diffuse fluorescence within the cell (Fig. 3A, Movie S3). Fluorescence inside the cell was dispersed as the dye molecules were released from ejected phage DNA and then bound to the bacterial chromosome; this is similar to comparable experiments with phage λ (Van Valen *et al*., 2012) and P22 (Mosier-Boss *et al*., 2003). Quantification of the fluorescence intensity at each time point is shown in the panels below each fluorescence micrograph (Fig. 3A). We measured the average time elapsed after mixing phage and bacteria until DNA transfer occurred for Sf6 bound to cells (Fig. 3B). Each data point in Fig. 3B represents a single Sf6 DNA ejection event, and the data are grouped into

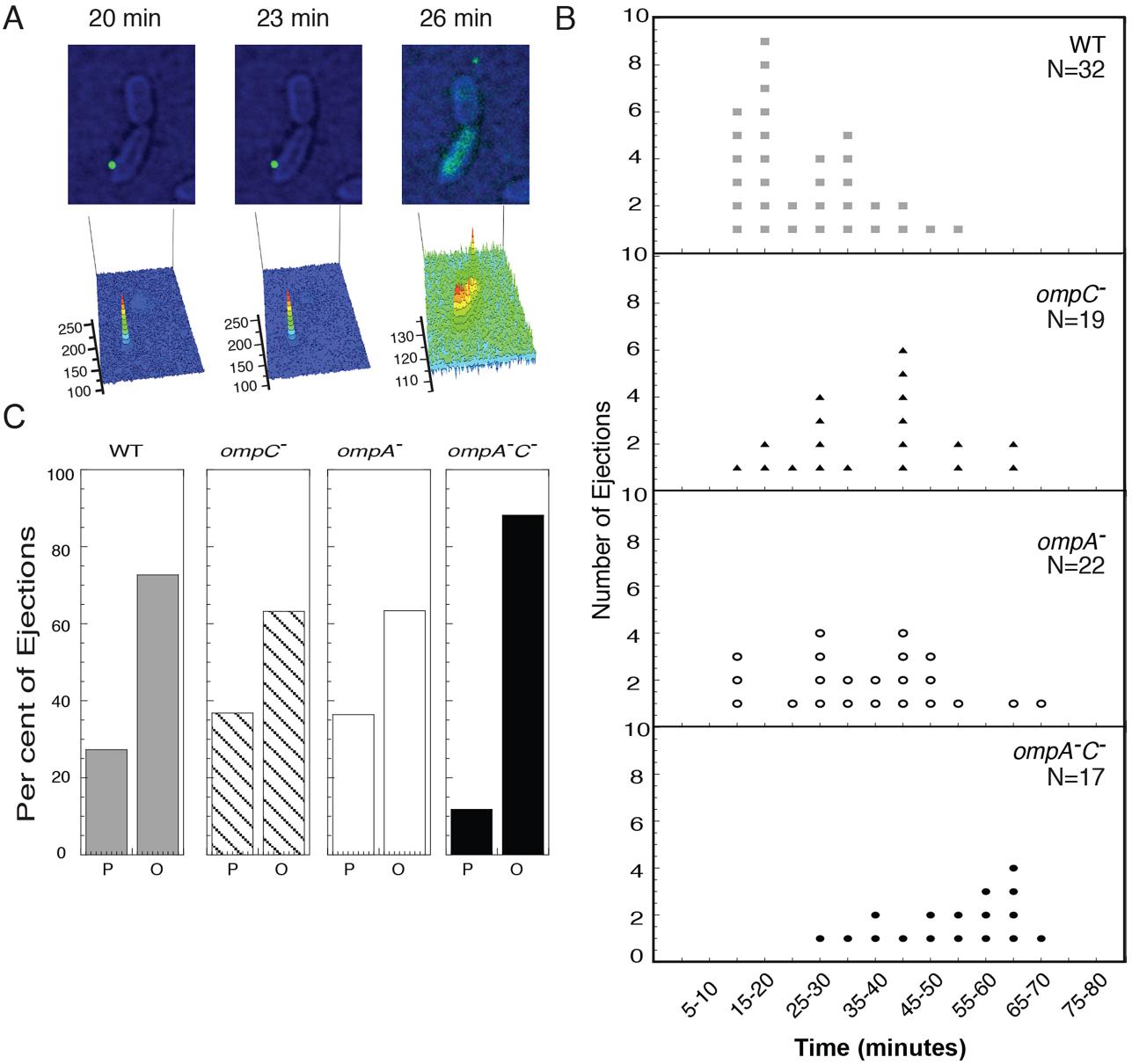

Fig. 3. Time-lapse fluorescence microscopy shows that Sf6 infection is slower on *omp* null strains.
A. Still frames of a time-lapse experiment showing Sf6 (labelled with Sytox green dye) attached to unstained, live WT *Shigella* (artificially coloured to enhance visibility). Below each still image is a schematic showing the pattern of fluorescence intensity of the Sytox signal in the frame.
B. Distribution of single particle results showing time of genome ejection post initiation of infection. Each dot represents a single phage-infection event.
C. Distribution of phage infection location. P ('at the pole'), is defined as phage infection observed in the quadrant nearest either pole and O ('regions other than the pole') is defined as the middle two quadrants of the cells that are not near the poles.

5 min bins. Phage infecting WT *Shigella* exhibited the shortest time between adsorption and DNA transfer (average of ~ 25 min, $n = 32$). The average time to ejection increased for the *omp* null strains, with the double knockout showing the longest delay (*ompA*$^-$, 36 min, $n = 22$; *ompC*$^-$, 36 min $n = 19$; *ompA*$^-$*C*$^-$, 52 min, $n = 17$). There is a large distribution in the times to ejection for individual virions infecting each strain, a similar phenomenon was also observed during *in vivo* fluorescence imaging of phage λ infecting *E. coli* (Van Valen *et al.*, 2012). We performed a T-test to validate that the observed average variation in ejection times was significant between strains. Injection times into the WT strain were significantly different than either of the single mutants or of the double mutant. The

resulting *P* values are as follows: WT versus *ompA*$^{-}$*C*$^{-}$, $P \leq 0.0001$ (t(47) = –7.57); WT versus *ompA*$^{-}$, $P = 0.002$ (t(52) = –3.25); WT versus *ompC*$^{-}$, $P = 0.0031$ (t(49) = –3.11); and *ompA*$^{-}$ versus *ompC*$^{-}$, $P = 0.96$ (t(39) = –0.055). The average times to ejection are slower than the eclipse measured in burst experiments (Fig. 2A), likely owing to differences in experimental design. For example, the fluorescence time-lapse experiments are performed at lower temperatures and with specimens immobilized on agar pads, versus higher temperatures and liquid culture as was used for the burst experiments.

We also examined the data to determine if there is a preferred site of infection on the cell surface, since phages SPP1, λ, T4, T7, P1, KVP40, and ϕA1122 are reported to preferentially infect cells at the poles (Edgar *et al*., 2008; Jakutyte *et al*., 2011). Sf6 showed no obvious preference for infections to initiate near cell poles for any of the strains tested (Fig. 3C). In instances involving infection of the null mutants of *S. flexneri*, adsorbed Sf6 virions appeared to diffuse along or 'scan' the surface until a suitable locus for infection was found (Movie S4). In many cases the phage were observed to continually scan the cell surface for the entire duration of the fluorescence microscopy experiments. However, a small fraction of phage were observed to infect the *ompA*$^{-}$*C*$^{-}$ cells, and the times until infection for these phage are reported in Fig. 3B. Our results are consistent with experiments performed using phage λ that demonstrate a target-finding process (Rothenberg *et al*., 2011). As a negative control, a mixture of Sf6 and *E. coli* MG1655 cells (lacking O-antigen and are not hosts for Sf6) was imaged; as expected, Sf6 did not absorb to or infect these cells (data not shown).

OMVs co-purify with Sf6 when grown on WT, ompA^{-}*, and ompC*$^{-}$ Shigella *strains, but not on an ompA*$^{-}$*C*$^{-}$ *strain*

As established in the above experiments, Sf6 infection kinetics are altered when OmpA and OmpC are absent. Previously, it was shown that OmpA and OmpC proteins co-purify with Sf6 virions, even after CsCl purification (Casjens *et al*., 2004; Zhao *et al*., 2011), and these proteins were subsequently shown be present in OMVs that appeared to be attached to the phage tails (Parent *et al*., 2012). It was unclear whether this association resulted from specific interactions between the Sf6 tail and the Omps or from other interactions with the lipid membrane. Therefore, we purified Sf6 virions propagated on WT, *ompA*$^{-}$, *ompC*$^{-}$, and *ompA*$^{-}$*C*$^{-}$ *S. flexneri*, by CsCl step gradient density centrifugation, and analysed the composition of each sample by cryo transmission electron microscopy (cryo-TEM) at low magnification (Fig. S5) and determined the relative amounts of co-purified OMVs when phage were grown on WT and on *omp* null strains. We inspected images of Sf6 purified from the different hosts and quantified the number of virions and the number of OMVs present in several preparations of each particle type (data not shown). This measure of the relative amounts of OMVs and phage is imprecise because it doesn't account for heterogeneity in OMV diameters, but it does provide a reasonable estimate of the relative differences. Phage propagated on *ompA*$^{-}$*C*$^{-}$ had significantly decreased levels (> 5-fold) of associated OMVs, compared to the WT, *ompA*$^{-}$, and *ompC*$^{-}$ strains. As negative controls, we analysed similar preparations of P22 and CUS-3 virions, which are not expected to co-purify with OMVs, and indeed we did not observe OMVs in these samples (data not shown). These results demonstrate that OmpA or OmpC is required for efficient physical association of OMVs with Sf6. Although virions could in theory associate through tailspike interaction with OMV LPS, the fact that few OMVs bind in the absence of both OmpA and OmpC suggests that this is not sufficient and that direct virion-Omp protein contact may be required.

Cryo-electron tomography of Sf6 bound to OMVs implies that the tail needle knob may interact with OmpA and OmpC

To gain direct visual evidence concerning the interactions between phage and host-derived membranes, we analysed Sf6 co-purified with OMVs from WT *S. flexneri* by cryo-electron tomography (Fig. 4). In all 54 tomographic volumes that were reconstructed, we observed a mixed population of particles among a total of 537 phage particles. The majority of these particles ($n = 312$), identified as 'free' virions, clearly had no interaction with any OMV. The others appeared to lie in close proximity to the vesicles, each with its tail apparatus interposed between the capsid and the host outer membrane, which suggests that Sf6 associates with the OMVs via their tail machinery. A subpopulation of these adsorbed particles ($n = 170$) contained high density inside the capsid ('full' virions), and the rest ($n = 55$) showed low density inside the capsid ('empty virions'), indicating they had released their genome. In the raw (i.e. unaveraged) tomograms (Movie S6), it was not possible to determine accurately the conformation of the tail apparatus. This is likely owing to the high level of noise and the resolution anisotropy caused by the 'missing wedge' effect (Frank, 2006), an artefact intrinsic to tomographic reconstructions because samples cannot be tilted a full ± 90 degrees in the microscope, and thus are only observed from a limited range of views. Therefore, we computed a sub-tomogram average for each subpopulation by extracting individual particle sub-volumes from the tomograms and aligning them to a common reference. As a control for assessing the quality of the reconstructions, we compared each of them to an asymmetric map of the

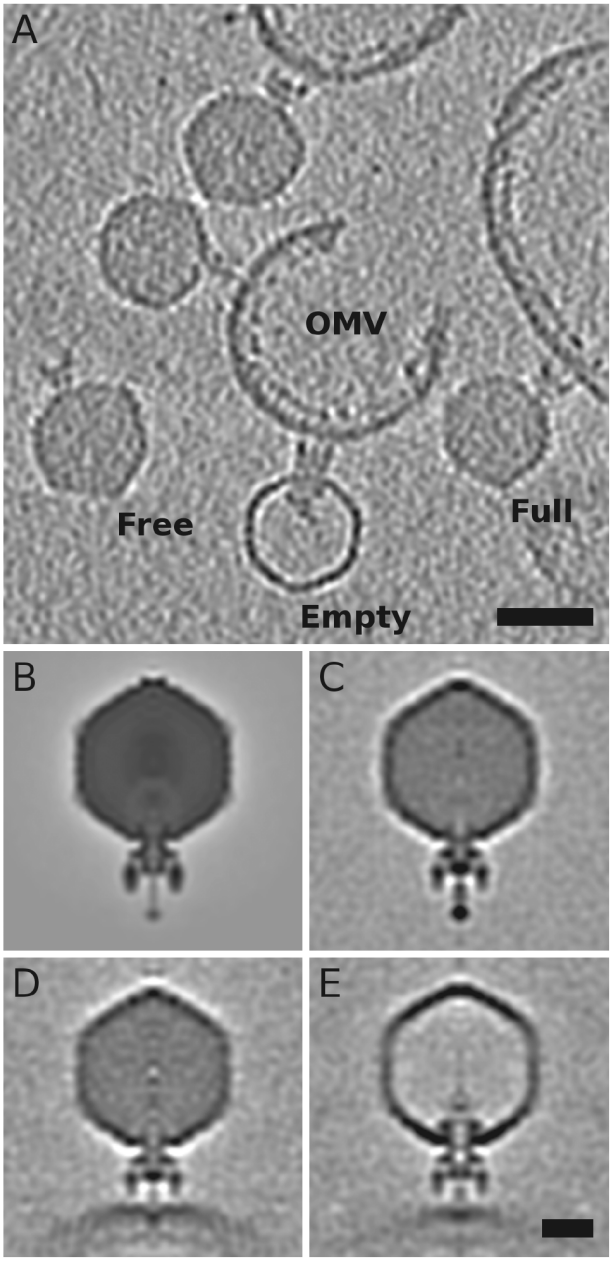

Fig. 4. Cryo-electron tomography and sub-tomogram averages of Sf6 'infecting' OMVs from *S. flexneri*.
A. A 40 Å thick slice from a representative 3D tomogram, showing isolated, unattached phage ('Free'), genome-containing phage that are attached to OMVs ('Full'), and genome-lacking phage attached to OMVs ('Empty'). Scale bar = 500 Å.
B. A planar, 5.85 Å thick, central section from a density map of Sf6 (filtered to 50 Å resolution, EMDB-5730) calculated by means of single particle, asymmetric reconstruction methods (Parent *et al*., 2012).
C–E. Same as panel (B) but for sub-tomogram averages of 'Free' (C), 'Full' (D), and 'Empty' (E) particles.
Scale bar for B–E = 200 Å.

Sf6 virion (EMDB-5730, Fig. 4B), which was previously reconstructed by single particle methods to 16 Å resolution (Parent *et al*., 2012). Aside from differences in resolution, the averaged 'free' virion sub-tomogram (Fig. 4C) compares quite well with the published model. Both capsids share the same structural features, and the tail apparatus adopts the same overall conformation. The sub-tomographic averages of the 'full' (Fig. 4D) and 'empty' (Fig. 4E) virions do not reveal any dramatic conformational differences, indicating that cell attachment and genome transfer can occur without extensive rearrangements of the phage tail. Furthermore, all the components of the tail apparatus are visible in the sub-tomogram averages, including the needle and its distal knob, which appears to insert into and indent the membrane.

Sf6 in vitro *genome ejection requires both LPS and an outer membrane protein*

OmpA and OmpC clearly influence Sf6 infection *in vivo*. Hence, we hypothesized that genome ejection *in vitro* might also require an Omp protein. For phage P22, purified LPS alone is sufficient to induce genome release *in vitro* (Andres *et al*., 2010; 2012). Therefore, we determined whether this is also true for Sf6. LPS was extracted from *S. enterica* serovar Typhimurium strain DB7136 and from *S. flexneri* serotype Y strain PE577 (see *Experimental procedures*). *In vitro* genome ejection was initiated by mixing phage particles and purified LPS (P22 was incubated with *S. enterica* serovar Typhimurium LPS, and Sf6 was incubated with *S. flexneri* serotype Y LPS), followed by incubation at 37°C for 120 min, as described (Andres *et al*., 2010; 2012). Phage genome release was confirmed by titring the remaining phage (Fig. 5A), negative stain electron microscopy (data not shown), and agarose electrophoresis gels that separate intact capsids and ejected genome stained with ethidium bromide (data not shown).

As was previously reported (Andres *et al*., 2010; 2012), purified *Salmonella* LPS was found to be sufficient for phage P22 genome release for the vast majority of virus particles as less than 10% intact P22 virions remained. In contrast, essentially all Sf6 virions remained intact after incubation with *Shigella* LPS, indicating that LPS alone is not sufficient for Sf6 genome release. To determine the contribution of OmpA to Sf6 *in vitro* ejection, we expressed and purified the transmembrane domain of *S. flexneri* OmpA ('OmpA-TM', residues 1–175, an 8-stranded β-barrel; this protein is missing its periplasmic long C-terminal domain) from *E. coli* inclusion bodies, and refolded the truncated protein in detergent micelles (see *Supporting information*). Similar to what was observed for LPS, the OmpA-TM domain alone was not sufficient for Sf6 genome ejection *in vitro*. However, in the presence of both LPS and OmpA-TM, ~ 95% of Sf6 virions released their

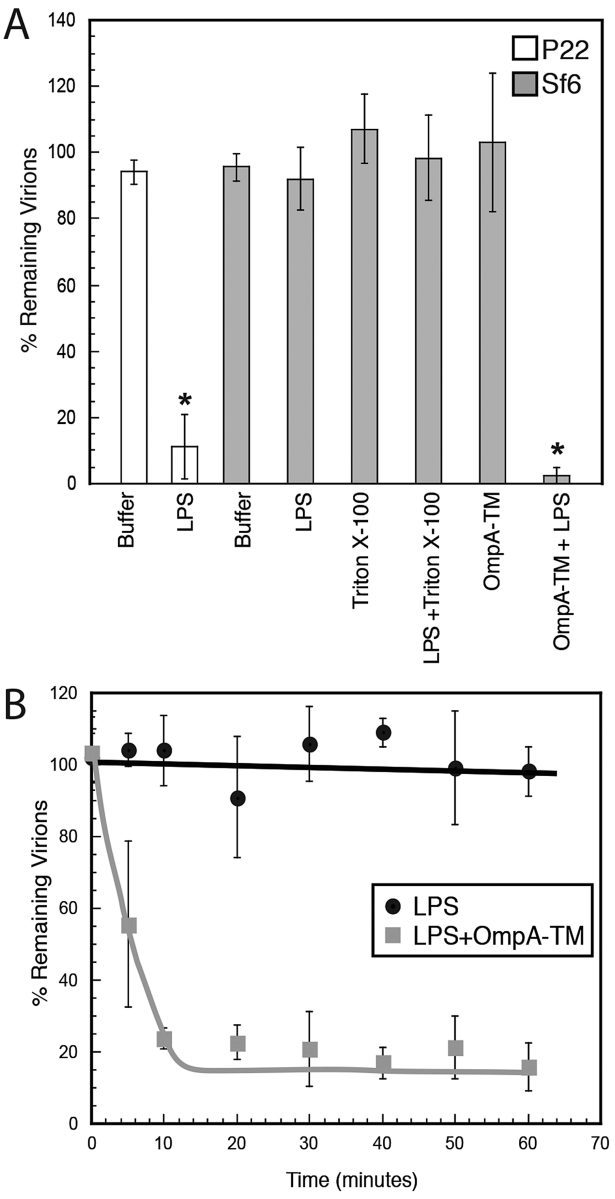

Fig. 5. *In vitro* genome ejection of Sf6 and P22.
A. '% Remaining Virions' was calculated as the number of pfu remaining after incubation with detergent, LPS, OmpA-TM, or LPS and OmpA-TM, divided by the number of pfu when incubated with buffer. The asterisks are there to emphasize the statistically significant data points (*i.e.* those conditions that resulted in *in vitro* genome release for Sf6 and P22).
B. '% Remaining Virions' was calculated at each time point as the number of pfu remaining after incubation with LPS or LPS and OmpA-TM, divided by the number of pfu when incubated with buffer at t = 0 min. Each data point is an average of at least three experiments, and the error bars signify one standard deviation.

genomes (Fig. 5A). To track Sf6 ejection rates, intact virions remaining in the Sf6 *in vitro* reactions were monitored for number of plaque-forming units. In the presence of OmpA-TM and LPS, functional virions are lost within 10 min, which is a physiologically relevant timescale. This suggests that, for Sf6, *in vitro* DNA release accurately reflects the natural infection (Fig. 5B). These experiments showed no difference when performed with LPS extracted from WT or the three omp null *Shigella* strains (data not shown).

Discussion

Primary and secondary phage receptors

A large number of specific protein–protein interactions must occur between virus-encoded and host-encoded proteins during intracellular multiplication. Phage virions recognize surface features that are diagnostic of each host cell in order to avoid non-productive infections. For tailed phages this recognition usually occurs in two stages: an initial and reversible stage in which the virion interacts with its primary receptor and a second, usually irreversible, stage since the virion must avoid non-productive ejection before it reaches the surface of the cell's outer membrane (Casjens and Molineux, 2012; Davidson *et al.*, 2012; Leiman and Shneider, 2012). It is often found that different virion proteins interact with primary and secondary receptors. T4 long tail fibres recognize the LPS core and/or OmpC protein as a primary receptor and its short tail fibres subsequently also recognize part of the core region of LPS (Riede, 1987; Thomassen *et al.*, 2003) as the secondary receptor. Phage Ox2 (a T4-like phage) tail fibre mutations that cause the fibres to bind to several different alternative primary receptor molecules do not affect the use of the secondary receptor (Drexler *et al.*, 1991), so these two interactions do not apparently need to be precisely spatially coupled. On the other hand, for phages λ, T5, and SPP1, interaction between the long tail fibre and primary receptor is not essential in the laboratory (Saigo, 1978; Heller and Braun, 1979; Hendrix and Duda, 1992; Baptista *et al.*, 2008). DNA delivery by podoviruses is particularly poorly understood, and in no case are both the primary and the secondary receptors known.

Sf6 displays different receptor binding requirements from P22

Sf6 and P22 are related members of the *Podoviridae* family, and their virions are built from similar structural proteins (Casjens *et al.*, 2004). However, our data suggest that they have different receptor requirements for productive infection. Recent work has identified LPS as the sole requirement for *in vitro* genome release for P22 (Andres *et al.*, 2010) as well as siphovirus 9NA (Andres *et al.*, 2012). For P22, this release rate *in vitro* is quite slow (> 60 min). Phage 9NA demonstrates faster release rates that match values for *in vitro* ejection by other phages such as λ and T5, where ejection is complete in a few minutes when triggered with purified LamB (Novick and

Baldeschwieler, 1988; Evilevitch *et al*., 2003; Grayson *et al*., 2007) or FhuA (Mangenot *et al*., 2005; Chiaruttini *et al*., 2010) respectively. The release rates reported for P22 reveal a discrepancy, as phage genome ejection happens in a few minutes, not several hours, *in vivo*. We have confirmed the slow P22 genome release results here as a comparison for our Sf6 studies. LPS alone is not sufficient for genome release in Sf6. In addition, Sf6 interactions with OmpA-TM alone are not enough to trigger genome release, but DNA is released in the presence of both LPS and OmpA-TM. The *in vitro* rates under these conditions are similar to preliminary observations of *in vivo* ejection rates (faster than 10 min by time-lapse fluorescence microscopy, data not shown). We propose that primary hydrolysis of LPS followed by a secondary interaction with Omps are needed to promote a productive Sf6 infection. The combination of the data presented here indicates that Sf6 requires interactions with a secondary receptor (OmpA or OmpC) for genome ejection.

OmpA and OmpC are receptors for many phages, including Sf6

OmpA is a major component of enterobacterial outer membranes, with ~ 100 000 copies presented on the surface of each cell (Koebnik *et al*., 2000). OmpA has ~ 99.6% identity between *E. coli* and *S. flexneri* (Power *et al*., 2006) and may present an alternative or accessory cell recognition mechanism for some members of the P22-like phages. OmpC has also been implicated as an essential receptor for bacteriophages PP01 (Mizoguchi *et al*., 2003), Gifsy-1/Gifsy-2 (Ho and Slauch, 2001a), and AR1 (Yu *et al*., 2000). In other instances, deletion of *ompC* decreases but does not eliminate phage sensitivity, indicating that OmpC may be one of several possible receptors, or may function as a co-receptor (Montag *et al*., 1989; Tanji *et al*., 2008). As reported here, it appears that OmpA is the preferred receptor for Sf6.

If OmpA and OmpC are the only secondary receptors for Sf6, the *ompA*$^{-}$*C*$^{-}$ double mutant should be completely resistant to Sf6 infection, and Sf6 virion preparations (as described above) might be expected not to have even the < 20% level of bound *omp*$^{-}$ OMVs. Why is Sf6 eventually able to infect *ompA*$^{-}$*C*$^{-}$ *Shigella*, albeit much more slowly than WT *Shigella*, and why are some virion-bound vesicles present after an *ompA*$^{-}$*C*$^{-}$ infection? Phage infection is a robust, dynamic process, and another membrane protein might be able to substitute for OmpA and OmpC. As described previously, OmpA and OmpC are the major protein components found in OMVs that co-purify with Sf6 virions, and this corresponds to the prominent bands seen in Coomassie-stained SDS-PAGE from 'purified' virions (Zhao *et al*., 2011; Parent *et al*., 2012). Mass spectrometry of such Sf6 virion preparations (Parent *et al*., 2012), also identified other outer membrane proteins, including OmpX and OmpF, but at much lower abundance than OmpA or OmpC. It is also possible that Sf6 can infect cells at sites of membrane defects when OmpA and OmpC are absent, which would correspond to the much slower rate and efficiency as observed by the fluorescence microscopy experiments on the *ompA*$^{-}$*C*$^{-}$ null host.

OmpA (Morona *et al*., 1984; Smith *et al*., 2007), OmpC (Yu and Mizushima, 1982; Ho and Slauch, 2001b; Mizoguchi *et al*., 2003), OmpX (Drexler *et al*., 1991), OmpF (Meyer *et al*., 2012), LamB (Randall-Hazelbauer and Schwartz, 1973), and FhuA (Braun and Wolff, 1973) have each been implicated as host receptors for various tailed phages. These proteins all have homologous folds made up of transmembrane β-barrels and surface-exposed loops, although their diameters and oligomeric states differ (Koebnik *et al*., 2000). Several studies have shown that phage have the ability to switch between a preferred receptor to an alternative one as a consequence of mutation (such as caused by a mutagen or culture environment) (Nguyen *et al*., 2012). A study of phage Ox2 host range mutants of *E. coli* showed that Ox2 can utilize OmpC for infection when OmpA is deleted (Morona and Henning, 1984). In a more recent study that monitored co-evolution of phage and hosts (Meyer *et al*., 2012), phage λ was able to recognize OmpF when LamB was absent and several mutations arose in the λJ protein. Therefore, given the prevalence and structural similarities of Omps, it is possible that, when OmpA is absent, Sf6 can recognize and bind to other Omps, such as OmpC. This apparent flexible use of receptors by phages should provide evolutionary advantages and adds another layer of complexity to the interactions between host and virus and could have implications for the use of phage in industrial and medical settings.

Cryo-electron tomograms indicate that Sf6 may bind OmpA and OmpC via the tail needle knob

Cryo-electron tomography has emerged as a very powerful tool for understanding complex phage architecture and binding to isolated membrane vesicles or hosts (Guerrero-Ferreira and Wright, 2013). Recent cryo-tomography work on *Podoviridae* interactions with hosts include studies of P-SSP7 (Liu *et al*., 2010) and T7 (Hu *et al*., 2013). These two phages are similar in structure, and both have an inner core and tail *fibres* (not tailspikes) that undergo extensive rearrangements upon docking to mini-cell surfaces. Alternatively, as presented here, Sf6 has large tailspike proteins that do not appear to undergo similar flexible and dramatic motions when docking to OMVs (Fig. 4). It is possible that small-scale rearrangements do occur in Sf6 tailspike proteins upon interaction with OMVs, but at the current resolution limits of

cryo-tomography (4–5 nm for these samples) we cannot detect such changes. However, at such low resolution, we do observe an indentation in the OMVs that corresponds to the apparent point of contact of the Sf6 tail needle with the membrane, mediated by the distal tip (knob domain). The tail needle knob, which is present in Sf6 but is remarkably absent in other phages like P22, has a tertiary structure (Olia *et al*., 2007) with a fold that is similar to virus receptor proteins in adenovirus and PRD-1 (Bhardwaj *et al*., 2011). Therefore, we propose that the tail needle knob in Sf6 is a likely candidate for interacting with *Shigella* OmpA and OmpC proteins when the phage approaches the cell membrane.

The needle tips of the 164 known, P22-like phage genomes are present as one of two non-homologous types; 69 have tip domains that are homologous with the Sf6 needle and 95 are homologous to the P22 needle tip (Casjens and Thuman-Commike, 2011; Leavitt *et al*., 2013). The P22-type tips are rather diverse, with the more divergent pairs being about 50% identical in amino acid sequence, whereas the Sf6-type tips are all > 95% identical to one another. The simplest explanation for this is that the P22-type tip is ancestral within this phage group, and the Sf6-type tip has much more recently introgressed into this population, but has not yet had time to diverge much since its arrival in the group (Leavitt *et al*., 2013). Such successful introgression implies that the Sf6-type tip confers an advantage to some phages over the P22-type tip under some circumstances. To date, the Sf6-type tip has only been found in phages that infect *Shigella* or *E. coli*, and not in phages that infect *Salmonella*, suggesting that it may give a special evolutionary advantage in the infection of the former species.

Experimental procedures

Single step growth curves

Shigella flexneri (WT, *ompA*$^-$, *ompC*$^-$, and *ompA*$^-$*C*$^-$) were grown in LB at 30°C to a concentration of 2×10^8 cells per ml. Phage infection was initiated at an moi of 15 for the WT, *ompA*$^-$, and *ompC*$^-$ strains, and an moi of 30 was used for the *ompA*$^-$*C*$^-$ strain. At times ranging from 0 to 3 h after infection was initiated, aliquots of infected cells were diluted with phage buffer containing saturating amounts of chloroform to lyse the cells. Lysates were plated and the number of phage per cell at each time point was calculated as described previously (Parent *et al*., 2004). Aliquots of the cells were assayed before infection and 10 min post infection to ensure that > 95% of the cells were infected, and therefore burst size determination was not affected by a second round of infected cells. These experiments were repeated in triplicate and representative plots are shown in Fig. 2A.

Adsorption rates of Sf6 to Shigella

Initial Sf6 adsorption to *Shigella* was monitored by adding phage to cells at high moi, taking aliquots at various times (ranging from zero to 20 min at 30°C), spinning out the cells and attached phage for 30 s in a microfuge, and titring the supernatant. The concentration of phage was held constant in each experiment (~ 1×10^9 phage per ml). We also accurately determined the cell concentration for each sample by plating and counting cfu before the addition of phage. The fit of these data was done using Kaleidagraph software and only data sets that demonstrated linear kinetics were included in further analysis.

Fluorescence microscopy

Fluorescent Sf6 were made by incubating a high-titre lysate ($\geq 10^9$ cfu ml^{-1}) with 1 μM of Sytox green nucleic acid stain at 4°C for 24 h. Overnight cultures of *Shigella flexneri* (WT, *ompA*$^-$, *ompC*$^-$, and *ompA*$^-$*C*$^-$) were diluted in LB and grown to mid-log at 30°C with aeration. Cells (1 ml) were pelleted with 1 min of centrifugation and resuspended in approximately 50 μl of fresh LB. Five microlitres of a DNase I mixture [two units DNase I (New England Biolabs), in 1× supplied DNase I buffer, in ddH_2O] were added to the cell re-suspension. A 5 μl aliquot of the cell suspension was mixed with 1 μl of Sytox-stained phage (at an moi < 10 phage per cell) and immediately spotted onto a thin, dried LB agar pad. Cells were incubated at room temperature for the duration of the experiment in order to increase the chances of capturing phage entry events. The earliest time point was taken within 3–5 min of phage addition and cells were imaged using DIC and FITC excitation for Sytox fluorescence, and images were recorded every 3 min for 1 h with a GE/Applied Precision Deltavision Elite System with an Olympus IX71 microscope and a 100 × 1.4 PlanApo lens.

High titre phage purification

Shigella flexneri (WT, *ompA*$^-$, *ompC*$^-$, and *ompA*$^-$*C*$^-$) were grown in LB at 37°C to 1×10^8 cells ml^{-1}. Sf6 infection was initiated at an moi of 0.1. The cultures were shaken until complete lysis occurred (~ 3.5 h at 37°C). A saturating amount of chloroform was added, and cell debris was removed by centrifugation (Sorvall SS-34 rotor, for 10 min at 10 000 r.p.m., 4°C). Phage were then concentrated at 18 000 r.p.m. for 90 min at 4°C. The resulting pellet was resuspended in phage buffer by nutation at 4°C overnight. Aggregated material was removed by centrifugation and the phage were further purified using a CsCl step gradient as described (Casjens *et al*., 2004), dialysed against phage buffer (10 mM Tris pH = 7.6, 10 mM $MgCl_2$), and concentrated to ~ 1×10^{14} phage ml^{-1} using a 30 MWCO micro concentrator (AMICON). Phage stocks were stored in phage buffer at 4°C.

Cryo-TEM

Small (3.5 μl) aliquots of purified phage were vitrified and examined using established procedures (Baker *et al*., 1999). Briefly, samples were applied to holey (Quantifoil) grids that had been glow-discharged for ~ 15 s in an Emitech K350 evaporation unit. Grids were then blotted with Whatman filter paper for ~ 5 s, plunged into liquid ethane, and transferred into a precooled FEI Polara, multi-specimen holder, which

maintained the vitrified specimen at liquid nitrogen temperature. Micrographs were recorded on a Gatan 4 K^2 CCD camera at 200 keV in an FEI Polara microscope at a nominal magnification of 19 542× (7.68 Å per pixel).

Cryo-electron tomography and sub-tomogram averaging

OMVs that co-purified with Sf6 from WT *Shigella* lytic infections were vitrified as described above, except with the addition of 5 nm gold beads (Sigma). Images were recorded at ~ 31 000× magnification at 200 keV in a tomographic, ± 60° tilt series using an FEI F20 microscope operated by Leginon (Potter *et al*., 1999), and images were collected at 2° tilt increments with a Gatan 4 K^2 CCD camera. Resulting tomograms were reconstructed using the IMOD program with the gold particles serving as fiducial markers (Kremer *et al*., 1996). We performed sub-tomogram averaging using routines previously implemented (Cardone *et al*., 2007), after some modifications tailored to this data set were made. Briefly, after computing 54 tomograms, we extracted from them sub volumes centred around 'free' virions, 'full' particles, and 'empty' particles. Initial orientations of the particles were estimated manually using the visualization program 3dmod in IMOD, and these served to generate an initial template without using any external reference. For each subvolume, a marker was placed on the phage tail machinery, and its position with respect to the centre of the sub-volume was used to align the particles so that all tails pointed in the same direction. The alignment was refined by iterative template matching, after masking a region just encompassing the tail machinery, to eliminate any contribution from the density of the capsid, without assuming or imposing any symmetry. Several iterations of refinement were performed by narrowing progressively the range allowed for the orientation parameters search until no improvement was observed both by Fourier shell correlation (FSC) calculations (van Heel and Schatz, 2005) and by visual inspection. The final maps, showing both capsid and tail machinery, were obtained by averaging the entire sub-volumes, with no mask applied, after aligning them according to the orientation parameters determined for the corresponding tails.

LPS extraction and in vitro *genome ejection*

LPS was extracted from overnight cultures of *S. typhimurium* and *S. flexneri* using a kit (BULLDOG BIO). LPS purity and concentration were determined by analysis of silver-stained tris-tricine SDS gels, dry weight, and absorbance spectra (data not shown). Phage were incubated with either purified LPS (solubilized in 10 mM Tris, pH = 7.6) derived from their respective host cells according to previous experiments (Andres *et al*., 2010), 150 μg ml^{-1} OmpA-TM (refolded in 1% triton X-100), or both LPS and OmpA-TM. The per cent remaining virions was calculated by dividing the pfu in each of the reactions by the pfu with only buffer added. For the time-course experiments, Sf6 phage were incubated with LPS or both LPS and OmpA-TM (150 μg ml^{-1}) as described above, and an aliquot was taken at each time point. The per cent remaining virions was calculated by dividing the pfu at each time point by the pfu with only buffer added. Plates were grown at 30°C with either DB7136 (P22) or PE577 (Sf6). Each histogram represents an average of at least three experiments, and the error bars signify one standard deviation.

Acknowledgements

We thank N. Olson (UCSD) for expert guidance in cryo-TEM methods, K. Willingford (UCSD) for counting statistics of Sf6 and OMVs from cryo-electron micrographs, J. Fredlund (Institut Pasteur) for advice on construction of the expression vector, and H. Hong (MSU) for advice on OmpA purification and refolding. This work was supported in part by NIH Grants R37 GM-033050 and 1S10 RR-020016 to TSB, AI074825 to SRC, R01 GM-073898 to JP, and support from UCSD and the Agouron Foundation to TSB to establish and support the UCSD cryo-TEM facilities. Some of the work presented here was conducted at the National Resource for Automated Molecular Microscopy, which is supported by the National Institutes of Health through the National Center for Research Resources' P41 programme (RR017573).

References

Allison, G.E., and Verma, N.K. (2000) Serotype-converting bacteriophages and O-antigen modification in *Shigella flexneri*. *Trends Microbiol* **8:** 17–23.

Ambrosi, C., Pompili, M., Scribano, D., Zagaglia, C., Ripa, S., and Nicoletti, M. (2012) Outer membrane protein A (OmpA): a new player in *Shigella flexneri* protrusion formation and inter-cellular spreading. *PLoS ONE* **7:** e49625.

Andres, D., Hanke, C., Baxa, U., Seul, A., Barbirz, S., and Seckler, R. (2010) Tailspike interactions with lipopolysaccharide effect DNA ejection from phage P22 particles *in vitro*. *J Biol Chem* **285:** 36768–36775.

Andres, D., Roske, Y., Doering, C., Heinemann, U., Seckler, R., and Barbirz, S. (2012) Tail morphology controls DNA release in two *Salmonella* phages with one lipopolysaccharide receptor recognition system. *Mol Microbiol* **83:** 1244–1253.

Aramli, L.A., and Teschke, C.M. (1999) Single amino acid substitutions globally suppress the folding defects of temperature-sensitive folding mutants of phage P22 coat protein. *J Biol Chem* **274**.

Baker, T.S., Olson, N.H., and Fuller, S.D. (1999) Adding the third dimension to virus life cycles: three-dimensional reconstruction of icosahedral viruses from cryo-electron micrographs. [Erratum appears in *Microbiol Mol Biol Rev* 2000; 64: 237.] *Microbiol Mol Biol Rev* **63:** 862–922.

Bamford, D.H., Grimes, J.M., and Stuart, D.I. (2005) What does structure tell us about virus evolution? *Curr Opin Struct Biol* **15:** 655–663.

Banks, D.J., Beres, S.B., and Musser, J.M. (2002) The fundamental contribution of phages to GAS evolution, genome diversification and strain emergence. *Trends Microbiol* **10:** 515–521.

Baptista, C., Santos, M.A., and Sao-Jose, C. (2008) Phage SPP1 reversible adsorption to *Bacillus subtilis* cell wall teichoic acids accelerates virus recognition of membrane receptor YueB. *J Bacteriol* **190:** 4989–4996.

Baxa, U., Steinbacher, S., Miller, S., Weintraub, A., Huber, R., and Seckler, R. (1996) Interactions of phage P22 tails with their cellular receptor, *Salmonella* O-antigen polysaccharide. *Biophys J* **71:** 2040–2048.

Berlanda Scorza, F., Colucci, A.M., Maggiore, L., Sanzone, S., Rossi, O., Ferlenghi, I., *et al*. (2012) High yield production process for *Shigella* outer membrane particles. *PLoS ONE* **7:** e35616.

Bhardwaj, A., Molineux, I.J., Casjens, S.R., and Cingolani, G. (2011) Atomic structure of bacteriophage Sf6 tail needle knob. *J Biol Chem* **286:** 30867–30877.

Botstein, D., Waddell, C.H., and King, J. (1973) Mechanism of head assembly and DNA encapsulation in *Salmonella* phage P22. I. Genes, proteins, structures and DNA maturation. *J Mol Biol* **80:** 669–695.

Braun, V., and Wolff, H. (1973) Characterization of the receptor protein for phage T5 and colicin M in the outer membrane of *E. coli* B. *FEBS Lett* **34:** 77–80.

Broadbent, S.E., Davies, M.R., and van der Woude, M.W. (2010) Phase variation controls expression of *Salmonella* lipopolysaccharide modification genes by a DNA methylation-dependent mechanism. *Mol Microbiol* **77:** 337–353.

Cardone, G., Winkler, D.C., Trus, B.L., Cheng, N., Heuser, J.E., Newcomb, W.W., *et al*. (2007) Visualization of the herpes simplex virus portal *in situ* by cryo-electron tomography. *Virology* **361:** 426–434.

Casjens, S., and Molineux, I. (2012) Short noncontractile tail machines: adsorption and DNA delivery by Podoviruses. In *Viral Molecular Machines*. Rossmann, M., and Rao, V. (eds). New York, NY: Springer, pp. 143–179.

Casjens, S., Winn-Stapley, D.A., Gilcrease, E.B., Morona, R., Kuhlewein, C., Chua, J.E., *et al*. (2004) The chromosome of *Shigella flexneri* bacteriophage Sf6: complete nucleotide sequence, genetic mosaicism, and DNA packaging. *J Mol Biol* **339:** 379–394.

Casjens, S.R., and Thuman-Commike, P.A. (2011) Evolution of mosaically related tailed bacteriophage genomes seen through the lens of phage P22 virion assembly. *Virology* **411:** 393–415.

Chiaruttini, N., de Frutos, M., Augarde, E., Boulanger, P., Letellier, L., and Viasnoff, V. (2010) Is the *in vitro* ejection of bacteriophage DNA quasistatic? A bulk to single virus study. *Biophys J* **99:** 447–455.

Chua, J.E., Manning, P.A., and Morona, R. (1999) The *Shigella flexneri* bacteriophage Sf6 tailspike protein (TSP)/endorhamnosidase is related to the bacteriophage P22 TSP and has a motif common to exo- and endoglycanases, and C-5 epimerases. *Microbiology* **145** (Part 7): 1649–1659.

Clark, C.A., Beltrame, J., and Manning, P.A. (1991) The *oac* gene encoding a lipopolysaccharide O-antigen acetylase maps adjacent to the integrase-encoding gene on the genome of *Shigella flexneri* bacteriophage Sf6. *Gene* **107:** 43–52.

Davidson, A.R., Cardarelli, L., Pell, L.G., Radford, D.R., and Maxwell, K.L. (2012) Long noncontractile tail machines of bacteriophages. *Adv Exp Med Biol* **726:** 115–142.

Drexler, K., Dannull, J., Hindennach, I., Mutschler, B., and Henning, U. (1991) Single mutations in a gene for a tail fiber component of an *Escherichia coli* phage can cause an extension from a protein to a carbohydrate as a receptor. *J Mol Biol* **219:** 655–663.

Edgar, R., Rokney, A., Feeney, M., Semsey, S., Kessel, M., Goldberg, M.B., *et al*. (2008) Bacteriophage infection is targeted to cellular poles. *Mol Microbiol* **68:** 1107–1116.

Evilevitch, A., Lavelle, L., Knobler, C.M., Raspaud, E., and Gelbart, W.M. (2003) Osmotic pressure inhibition of DNA ejection from phage. *Proc Natl Acad Sci USA* **100:** 9292–9295.

Feil, E.J. (2012) The emergence and spread of dysentery. *Nat Genet* **44:** 964–965.

Frank, J. (2006) *Electron Tomography: Methods for Three-dimensional Visualization of Structures in the Cell*, 2nd edn. New York; London: Springer.

Gemski, P., Jr, Koeltzow, D.E., and Formal, S.B. (1975) Phage conversion of *Shigella flexneri* group antigens. *Infect Immun* **11:** 685–691.

Gordon, C.L. (1993) Analysis of conditional-lethal mutations of the phage P22 coat protein. In *Biology*. Cambridge, MA: Massachusetts Institute of Technology.

Grayson, P., Han, L., Winther, T., and Phillips, R. (2007) Real-time observations of single bacteriophage lambda DNA ejections *in vitro*. *Proc Natl Acad Sci USA* **104:** 14652–14657.

Guerrero-Ferreira, R.C., and Wright, E.R. (2013) Cryo-electron tomography of bacterial viruses. *Virology* **435:** 179–186.

van Heel, M., and Schatz, M. (2005) Fourier shell correlation threshold criteria. *J Struct Biol* **151:** 250–262.

Heller, K., and Braun, V. (1979) Accelerated adsorption of bacteriophage T5 to *Escherichia coli* F, resulting from reversible tail fiber-lipopolysaccharide binding. *J Bacteriol* **139:** 32–38.

Hendrix, R.W., and Duda, R.L. (1992) Bacteriophage lambda PaPa: not the mother of all lambda phages. *Science* **258:** 1145–1148.

Ho, T.D., and Slauch, J.M. (2001a) OmpC is the receptor for Gifsy-1 and Gifsy-2 bacteriophages of *Salmonella*. *J Bacteriol* **183:** 1495–1498.

Ho, T.D., and Slauch, J.M. (2001b) OmpC is the receptor for Gifsy-1 and Gifsy-2 bacteriophages of *Salmonella*. *J Bacteriol* **183:** 1495–1498.

Holt, K.E., Baker, S., Weill, F.X., Holmes, E.C., Kitchen, A., Yu, J., *et al*. (2012) *Shigella sonnei* genome sequencing and phylogenetic analysis indicate recent global dissemination from Europe. *Nat Genet* **44:** 1056–1059.

Hu, B., Margolin, W., Molineux, I.J., and Liu, J. (2013) The bacteriophage t7 virion undergoes extensive structural remodeling during infection. *Science* **339:** 576–579.

Jakutyte, L., Baptista, C., Sao-Jose, C., Daugelavicius, R., Carballido-Lopez, R., and Tavares, P. (2011) Bacteriophage infection in rod-shaped gram-positive bacteria: evidence for a preferential polar route for phage SPP1 entry in *Bacillus subtilis*. *J Bacteriol* **193:** 4893–4903.

Kiino, D.R., Singer, M.S., and Rothman-Denes, L.B. (1993) Two overlapping genes encoding membrane proteins required for bacteriophage N4 adsorption. *J Bacteriol* **175:** 7081–7085.

Koebnik, R., Locher, K.P., and Van Gelder, P. (2000) Struc-

ture and function of bacterial outer membrane proteins: barrels in a nutshell. *Mol Microbiol* **37:** 239–253.
Kotloff, K.L., Winickoff, J.P., Ivanoff, B., Clemens, J.D., Swerdlow, D.L., Sansonetti, P.J., *et al*. (1999) Global burden of *Shigella* infections: implications for vaccine development and implementation of control strategies. *Bull World Health Organ* **77:** 651–666.
Kremer, J.R., Mastronarde, D.N., and McIntosh, J.R. (1996) Computer visualization of three-dimensional image data using IMOD. *J Struct Biol* **116:** 71–76.
Kulp, A., and Kuehn, M.J. (2010) Biological functions and biogenesis of secreted bacterial outer membrane vesicles. *Annu Rev Microbiol* **64:** 163–184.
Langsrud, S., and Sundheim, G. (1996) Flow cytometry for rapid assessment of viability after exposure to a quaternary ammonium compound. *J Appl Bacteriol* **81:** 411–418.
Leavitt, J.C., Gogokhia, L., Gilcrease, E.B., Bhardwaj, A., Cingolani, G., and Casjens, S.R. (2013) The tip of the tail needle affects the rate of DNA delivery by bacteriophage P22. *PLoS ONE* **8:** e70936.
Leiman, P.G., and Shneider, M.M. (2012) Contractile tail machines of bacteriophages. *Adv Exp Med Biol* **726:** 93–114.
Liu, X., Zhang, Q., Murata, K., Baker, M.L., Sullivan, M.B., Fu, C., *et al*. (2010) Structural changes in a marine podovirus associated with release of its genome into *Prochlorococcus*. *Nat Struct Mol Biol* **17:** 830–837.
MacConkey, A. (1905) Lactose-fermenting bacteria in faeces. *J Hyg (Lond)* **5:** 333–379.
McPartland, J., and Rothman-Denes, L.B. (2009) The tail sheath of bacteriophage N4 interacts with the *Escherichia coli* receptor. *J Bacteriol* **191:** 525–532.
Mangenot, S., Hochrein, M., Radler, J., and Letellier, L. (2005) Real-time imaging of DNA ejection from single phage particles. *Curr Biol* **15:** 430–435.
Meyer, J.R., Dobias, D.T., Weitz, J.S., Barrick, J.E., Quick, R.T., and Lenski, R.E. (2012) Repeatability and contingency in the evolution of a key innovation in phage lambda. *Science* **335:** 428–432.
Mizoguchi, K., Morita, M., Fischer, C.R., Yoichi, M., Tanji, Y., and Unno, H. (2003) Coevolution of bacteriophage PP01 and *Escherichia coli* O157:H7 in continuous culture. *Appl Environ Microbiol* **69:** 170–176.
Montag, D., Schwarz, H., and Henning, U. (1989) A component of the side tail fiber of *Escherichia coli* bacteriophage lambda can functionally replace the receptor-recognizing part of a long tail fiber protein of the unrelated bacteriophage T4. *J Bacteriol* **171:** 4378–4384.
Morona, R., and Henning, U. (1984) Host range mutants of bacteriophage Ox2 can use two different outer membrane proteins of *Escherichia coli* K-12 as receptors. *J Bacteriol* **159:** 579–582.
Morona, R., Klose, M., and Henning, U. (1984) *Escherichia coli* K-12 outer membrane protein (OmpA) as a bacteriophage receptor: analysis of mutant genes expressing altered proteins. *J Bacteriol* **159:** 570–578.
Mosier-Boss, P.A., Lieberman, S.H., Andrews, J.M., Rohwer, F.L., Wegley, L.E., and Breitbart, M. (2003) Use of fluorescently labeled phage in the detection and identification of bacterial species. *Appl Spectrosc* **57:** 1138–1144.
Muller, J.J., Barbirz, S., Heinle, K., Freiberg, A., Seckler, R., and Heinemann, U. (2008) An intersubunit active site between supercoiled parallel beta helices in the trimeric tailspike endorhamnosidase of *Shigella flexneri* Phage Sf6. *Structure* **16:** 766–775.
Nguyen, A.H., Molineux, I.J., Springman, R., and Bull, J.J. (2012) Multiple genetic pathways to similar fitness limits during viral adaptation to a new host. *Evolution Int J Org Evolution* **66:** 363–374.
Novick, S.L., and Baldeschwieler, J.D. (1988) Fluorescence measurement of the kinetics of DNA injection by bacteriophage lambda into liposomes. *Biochemistry* **27:** 7919–7924.
Olia, A.S., Casjens, S., and Cingolani, G. (2007) Structure of phage P22 cell envelope-penetrating needle. *Nat Struct Mol Biol* **14:** 1221–1226.
Parent, K.N., Ranaghan, M.J., and Teschke, C.M. (2004) A second site suppressor of a folding defect functions via interactions with a chaperone network to improve folding and assembly *in vivo*. *Mol Microbiol* **54:** 1036–1054.
Parent, K.N., Gilcrease, E.B., Casjens, S.R., and Baker, T.S. (2012) Structural evolution of the P22-like phages: comparison of Sf6 and P22 procapsid and virion architectures. *Virology* **427:** 177–188.
Poranen, M.M., Daugelavicius, R., and Bamford, D.H. (2002) Common principles in viral entry. *Annu Rev Microbiol* **56:** 521–538.
Potter, C.S., Chu, H., Frey, B., Green, C., Kisseberth, N., Madden, T.J., *et al*. (1999) Leginon: a system for fully automated acquisition of 1000 electron micrographs a day. *Ultramicroscopy* **77:** 153–161.
Power, M.L., Ferrari, B.C., Littlefield-Wyer, J., Gordon, D.M., Slade, M.B., and Veal, D.A. (2006) A naturally occurring novel allele of *Escherichia coli* outer membrane protein A reduces sensitivity to bacteriophage. *Appl Environ Microbiol* **72:** 7930–7932.
Randall-Hazelbauer, L., and Schwartz, M. (1973) Isolation of the bacteriophage lambda receptor from *Escherichia coli*. *J Bacteriol* **116:** 1436–1446.
Riede, I. (1987) Receptor specificity of the short tail fibres (gp12) of T-even type *Escherichia coli* phages. *Mol Gen Genet* **206:** 110–115.
Roth, B.L., Poot, M., Yue, S.T., and Millard, P.J. (1997) Bacterial viability and antibiotic susceptibility testing with SYTOX green nucleic acid stain. *Appl Environ Microbiol* **63:** 2421–2431.
Rothenberg, E., Sepulveda, L.A., Skinner, S.O., Zeng, L., Selvin, P.R., and Golding, I. (2011) Single-virus tracking reveals a spatial receptor-dependent search mechanism. *Biophys J* **100:** 2875–2882.
Saigo, K. (1978) Isolation of high-density mutants and identification of nonessential structural proteins in bacteriophage T5; dispensability of L-shaped tail fibers and a secondary major head protein. *Virology* **85:** 422–433.
Smith, S.G., Mahon, V., Lambert, M.A., and Fagan, R.P. (2007) A molecular Swiss army knife: OmpA structure, function and expression. *FEMS Microbiol Lett* **273:** 1–11.
Steinbacher, S., Miller, S., Baxa, U., Budisa, N., Weintraub, A., Seckler, R., and Huber, R. (1997) Phage P22 tailspike protein: crystal structure of the head-binding domain at 2.3A, fully refined structure of the endorhamnosidase at

1.56A resolution, and the molecular basis of O-antigen recognition and cleavage. *J Mol Biol* **267:** 865–880.

Tanji, Y., Hattori, K., Suzuki, K., and Miyanaga, K. (2008) Spontaneous deletion of a 209-kilobase-pair fragment from the *Escherichia coli* genome occurs with acquisition of resistance to an assortment of infectious phages. *Appl Environ Microbiol* **74:** 4256–4263.

Thomassen, E., Gielen, G., Schutz, M., Schoehn, G., Abrahams, J.P., Miller, S., and van Raaij, M.J. (2003) The structure of the receptor-binding domain of the bacteriophage T4 short tail fibre reveals a knitted trimeric metal-binding fold. *J Mol Biol* **331:** 361–373.

Van Valen, D., Wu, D., Chen, Y.J., Tuson, H., Wiggins, P., and Phillips, R. (2012) A single-molecule Hershey-Chase experiment. *Curr Biol* **22:** 1339–1343.

Verma, N.K., Brandt, J.M., Verma, D.J., and Lindberg, A.A. (1991) Molecular characterization of the O-acetyl transferase gene of converting bacteriophage SF6 that adds group antigen 6 to *Shigella flexneri*. *Mol Microbiol* **5:** 71–75.

Warren, B.R., Parish, M.E., and Schneider, K.R. (2006) *Shigella* as a foodborne pathogen and current methods for detection in food. *Crit Rev Food Sci Nutr* **46:** 551–567.

Yu, F., and Mizushima, S. (1982) Roles of lipopolysaccharide and outer membrane protein OmpC of *Escherichia coli* K-12 in the receptor function for bacteriophage T4. *J Bacteriol* **151:** 718–722.

Yu, S.L., Ko, K.L., Chen, C.S., Chang, Y.C., and Syu, W.J. (2000) Characterization of the distal tail fiber locus and determination of the receptor for phage AR1, which specifically infects *Escherichia coli* O157:H7. *J Bacteriol* **182:** 5962–5968.

Zhao, H., Sequeira, R.D., Galeva, N.A., and Tang, L. (2011) The host outer membrane proteins OmpA and OmpC are associated with the *Shigella* phage Sf6 virion. *Virology* **409:** 319–327.

Supporting information

Additional supporting information may be found in the online version of this article at the publisher's web-site.